Journal of the Korean Magnetic Resonance Society **2001**, *5*, 73-90

Location and Adsorbate Interactions of V(IV) Species in VH-SAPO-34 Studied by EPR and Electron Spin-Echo Modulation Spectroscopies

Gernho Back[+*], Young-Soo Cho[+], Yong-Ill Lee[+], Yanghee Kim[+], and Larry Kevan[++]

Department of Chemistry, Changwon National University, Changwon, Kyungnam, 641-773, Korea
Department of Chemistry, University of Houston, Houston, Texas 77204-5641[++]
Received September 7, 2001

Absracts: Vanadium-doped H-SAPO-34 samples were prepared by a high-temperature solid-state reaction between SAPO-34 and the paramagnetic V(IV) species and characterized carefully by EPR and Electron Spin-Echo Modulation(ESEM) studies. The paramagnetic vanadium species generated in both V_2O_5 and $VOSO_4$ of SAPO-34 have the same narrow range of g value for vanadium species assigned to VO^{2+} inferred from the isotropic EPR spectrum at 293 K. The EPR and ESEM data indicate that the V(IV) species exist as a vanadyl ion either as $[V(IV)]O^{2+}$ or V^{4+}. The $[V(IV)]O^{2+}$ species seems to be more probable because SAPO-34 having a low negative framework charge[35] and more positively charged species like V^{4+} can not be easily stabilized. Tetravalent vanadium ion in vadium-doped H- SAPO-34 can only be observed at the temperature lower than 77 K, while the vanadyl ion, VO^{2+} in the activated sample of VH-SAPO-34 can produce the ion even at room temperature. After the adsorption of methanol, ethanol, propanol or ethene to the VH-SAPO-34, only one molecule coordinate to $[V(IV)]O^{2+}$ was observed in EPR and ESEM spectra.

INTRODUCTION

Microporus crystalline aluminophophates($AlPO_4$-n) have been recently synthesized hydrothermally with morpholine being used as the templating agent.[1-3] Isomorphous substitution of several different elements into the $AlPO_4$-n framework can be possible, of which the framework phosphorus substitution by silicon is of particular importance for their applications, such as adsorbents for separation and purification of molecular species, catalysts, or catalyst supports, and ion-exchange agents.[4] It is well known that vanadium-loaded catalysts are useful for selective oxidation of hydrocarbons, such as *o*-xylene to phthalic anhydride[5,6]; and toluene to bezhaldehyde[7,8], the catalytic reduction of NO and NO_2 by ammonia in the presence of O_2,[9-11]. The active site of these reactions on the supported vanadium catalysts has been hypothesized to be the surface V=O species.[12] A number of attempts have been made to characterize the coordinatively unsaturated vanadium species

*To whom : ghback@sarim.changwon.ac.kr

on the supported catalyst, but very few quantitative results have been obtained.[13-17] Chon et al.[18] suggested that tetravalent vanadium in the calcined VAPO-$_5$ system is incorporated as V(IV) on the basis of chemical analysis and optical measurements. In recent years geometries of various adsorbates coordinated to vanadium species on silica have been determined by EPR method.[19] From the combined studies of EPR and ESEM it was concluded that tetravalent vanadium interacts with three methanol molecules in the first coordination sphere and with two methanol molecules in the second coordination sphere. However, there has been no published papers to characterize the structure of V(IV) in silicoaluminophophate(SAPO) molecular sieves clearly. In this work, vanadium-doped H-SAPO-34 samples were prepared by a high-temperature solid-state reaction between SAPO-34 and the paramagnetic V(IV) species and characterized carefully by EPR and ESEM studies.

EXPERIMENTAL

Synthesis and Solid-state ion exchange of SAPO-34 were carried out by a modification of the reported methods in the literature.[20,21] An aqueous solution (4.5 ml) of 85 % H_3PO_4(Mallinckrodt) was prepared by diluting the solution with 6.7 ml of de-ionized water and stirred for 10 min. After adding 7.7 ml of de-ionized water to the H_3PO_4 solution with continuous stirring, four portions (0.175 g for each time) of 0.7 g of $Al_2O_3.H_2O$ (Vista Chemical) were added successively every hour. The resulting homogeneous mixture was followed by successive addition of 0.20 g of fumed SiO_2 (Cab-O-Sil total 0.8 g fumed SiO_2) every 30 min over 2 h periods. Then, the mixture was cooled in ice water and 13.9 ml of triethylamine (Aldrich) was added dropwise followed by continuous stirring at room temperature. The solution was stirred overnight to give a bulk mole ratio of $Si_1Al_3P_5$. After about 14 h of stirring, the pH of the mixture was adjusted to 6.9 by the addition of 40 wt% HF solution (Aldrich). A Tefron-lined autoclave was filled to 50 % of its capacity with the synthesis mixture and heated to 200 °C and kept for 6 days.

Solid-state reaction of $VOSO_4.XH_2O$ and As-synthesized SAPO-34

The quantities, 0.010 g of $VOSO_4.XH_2O$ (Alfa) and 0.5 g of as-synthesized SAPO-34, were mixed with a mortar and pestle for about 30 min. The mixture was pressed in a stainless-steel die to make a pellet of 12 mm diameter and 2.5 mm thickness. The pellet was put in a quartz boat and heated in a furnace at 600 °C in O_2 and kept for 12 h. This calcined sample was cooled slowly to room temperature. Before and after this solid state reaction, the sample was white. Since this templating-free VH-SAPO-34 loses its crystallinity slowly with moisture, the samples were stored under vacuum.

Solid-state Reaction of V_2O_5 and As-synthesized SAPO-34

Another solid state reaction products of VH-SAPO-34 was prepared by the same procedure for the reaction between $VOSO_4.XH_2O$ and as-synthesized SAPO-34, starting

with mixing V_2O_5 and as-synthesized SAPO-34.

Sample Treatment

A hydrated VH-SAPO-34 was first loaded into 3 mm out diameter by 2mm inner diameter Suprasil quartz tubes and evacuated at room temperature. Evacuation was continued by slowly raising the temperature to 600 °C for 11 h where the temperature was maintained. The evacuated samples were heated under 230 Torr of dry oxygen at 600 °C for 3.5 h and then cooled to room temperature to give a dehydrated sample (Note the EPR spectrum in Figure 1b). The activated samples were exposed to liquid adsorbates(D_2O, CH_3OD, CD_3OH, C_2H_5OD, C_3H_7OD) at their room temperature vapor pressure or to gaseous adsorbates (ND_3 and C_2D_4) as specified in the figure captions. All adsorbates were obtained from Cambridge Isotope Laboratories. The sample tubes were sealed after exposu-

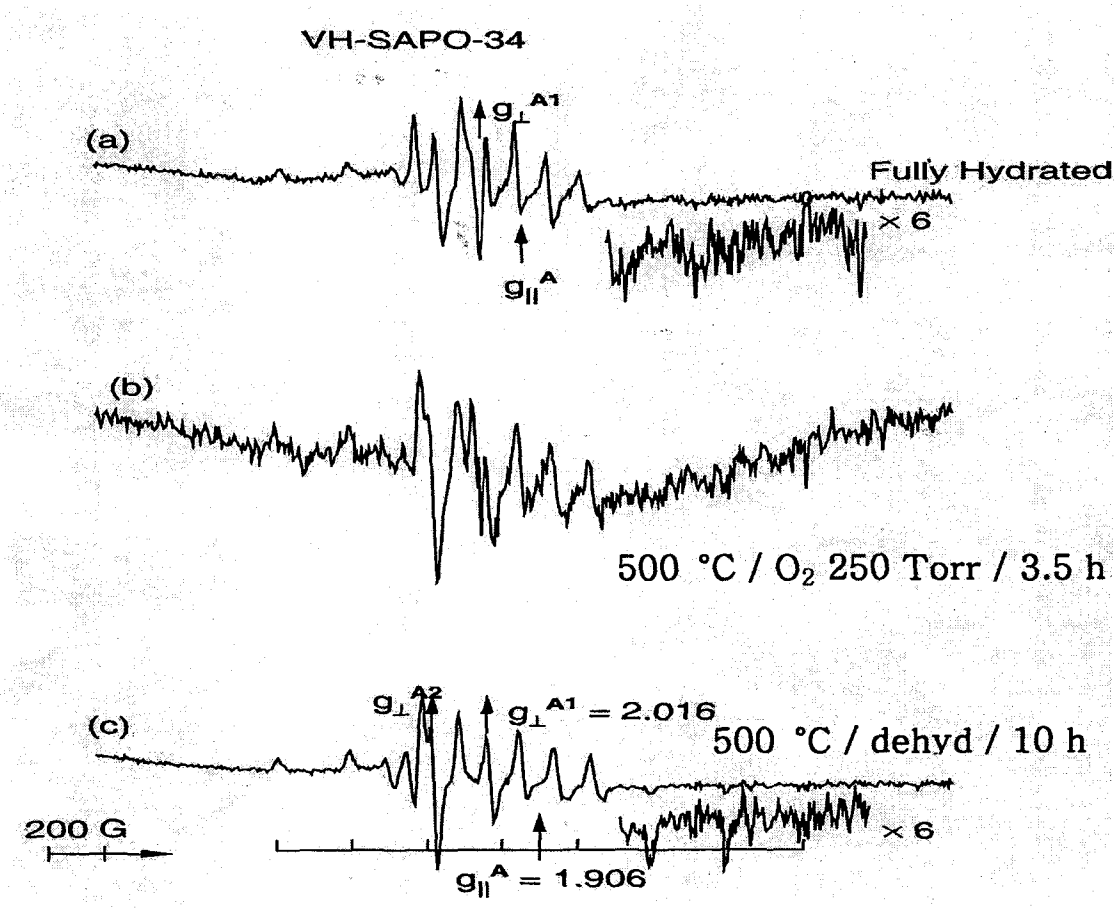

Fig. 1. EPR spectra at 77 K of activated VH-SAPO-34 (a) type A, after fully hydration at room temperature after calcinations at 600 °C for 12 h, (b) type B, after

re to adsorbates and were stored in liquid nitrogen. The dehydrated sample was heated subsequently in vacuum to 500 °C for about
10 h to give an activated sample (Figure 1c). The dehydrated sample showed a weak EPR signal, while the activated sample showed a strong EPR signal. subsequent oxidation with 250 Torr of dry oxygen at 500 °C for 3.5 h and degassing at room temperature, (c) after subsequent evacuation at 500 °C for 10 h.

Spectroscopic measurements

The V ion-exchange and calcinations of as-synthesized SAPO-34 were examined by the use of a powder X-ray diffraction(XRD) with a Phillips PW 1840 diffractometer. Thermogravimetric analysis were performed by a Dupon 951 thermal analyzer with heating rate of 10 °C min^{-1}. The EPR spectra were recorded with a modified Varian E-4 spectrometer interfaced to a Tracer Norton TN-1710 signal averager at 77 K. Each spectrum was obtained by multiple scan to achieve a satisfactory signal-to-noise-ratio. Each acquired spectrum was transferred from the signal averager to an IBM PC/XT compatible computer for analysis and plotting. The magnetic field was calibrated with a Varian E-500 gauss meter. The microwave frequency was measured at 4 K with a Bruker ESP 380 pulsed ESR spectrometer. Three pulse echoes were measured by using a 90 °-τ-90 °-T-90 ° pulse sequences with τ = 0.26~0.28 μs, and echo intensity was measured as a function of T. The theory and simulation of ESEM are described elsewhere.[23,24]

RESULTS

As-synthesized SAPO-34 and VH-SAPO-34 were well crystallized and their X-ray diffraction(XRD) spectra were shown in Figure 2 and 3.

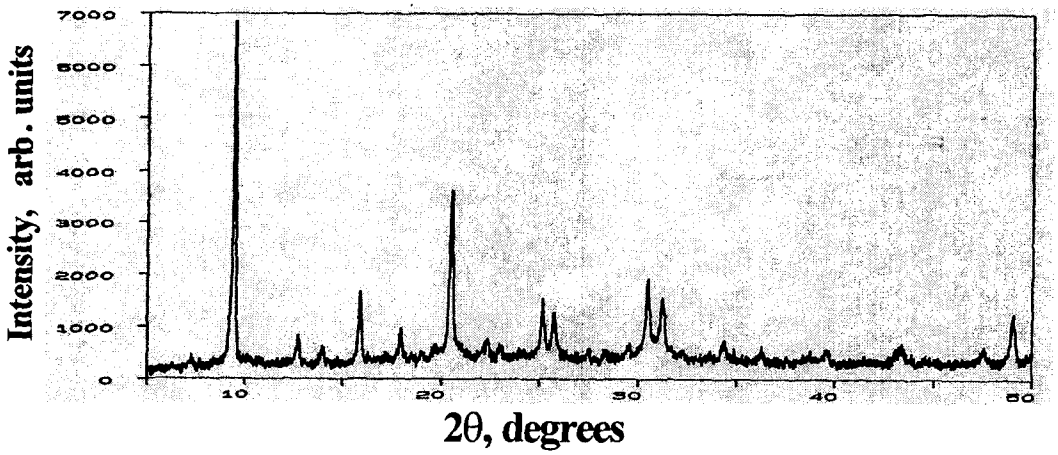

Fig. 2. XRD spectrum of as-synthesized SAPO-34.

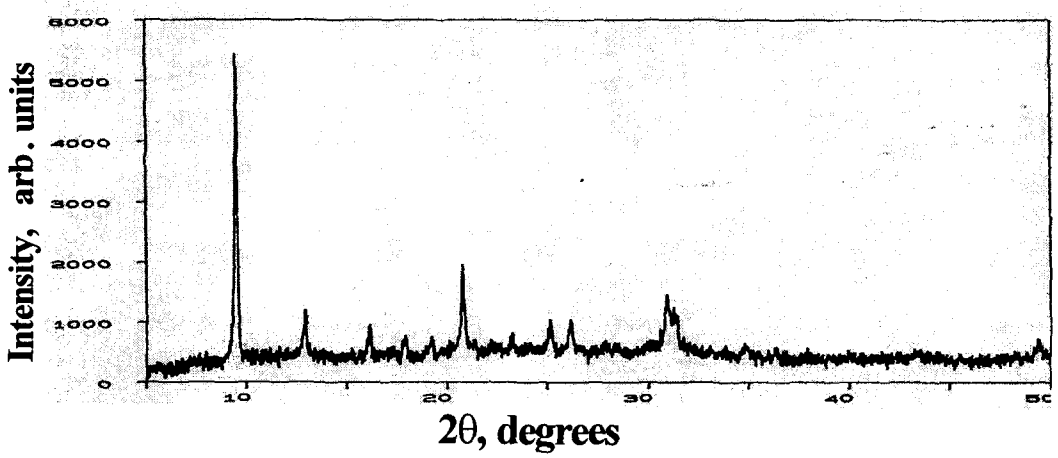

Fig. 3. XRD spectrum of calcined VH-SAPO-34.

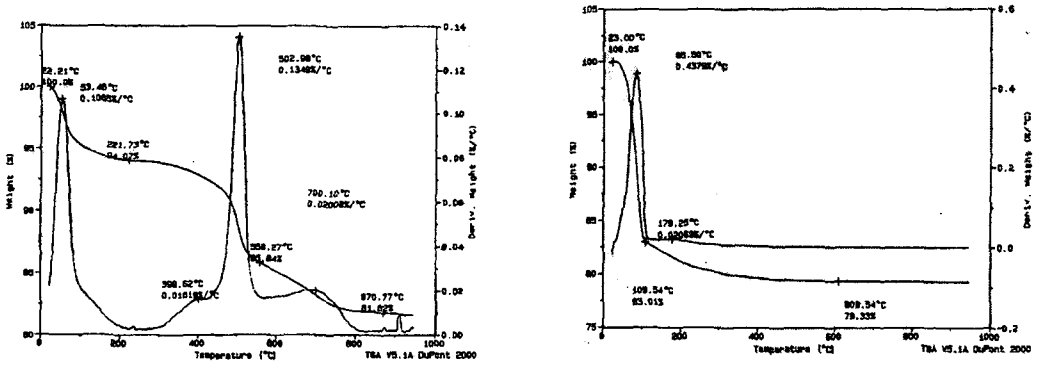

(a)소성전 (b) 소성후

Fig. 4. TGA (Thermogravimetric Analysis) spectra of as-synthesized SAPO-34(A) and calcined VH-SAPO-34(B).

There are no significant differences in XRD spectra between as-synthesized SAPO-34 and calcined VH-SAPO-34. Thermogravimetric analysis shows that as-synthesized SAPO-34 has different weight-losses around 400, 500, and 700 °C, compared to calcined H-SAPO-34 (see Figure 4a). These additional weight losses are probably due to the desorption or decomposition of the organic templating agent, triethylamine, which indicates the presence of acid sites. The calcined VH-SAPO-34 has a weight loss only around 100 °C during heating to 900 °C. This weight loss is probably due to the desorption of H_2O.

Electron Paramagnetic Resonance

The paramagnetic vanadium species generated in both V_2O_5 and $VOSO_4$ of SAPO-34 have the same narrow range of g value for vanadium species assigned to VO^{2+} inferred from the isotropic EPR spectrum at 300 K(see Figure 5a).

The observed eight-lined spectrum arises from the hyperfine interaction of the unpaired electron in $3d^1$ configuration with ^{51}V nucleus of nuclear spin $I = 7/2$.

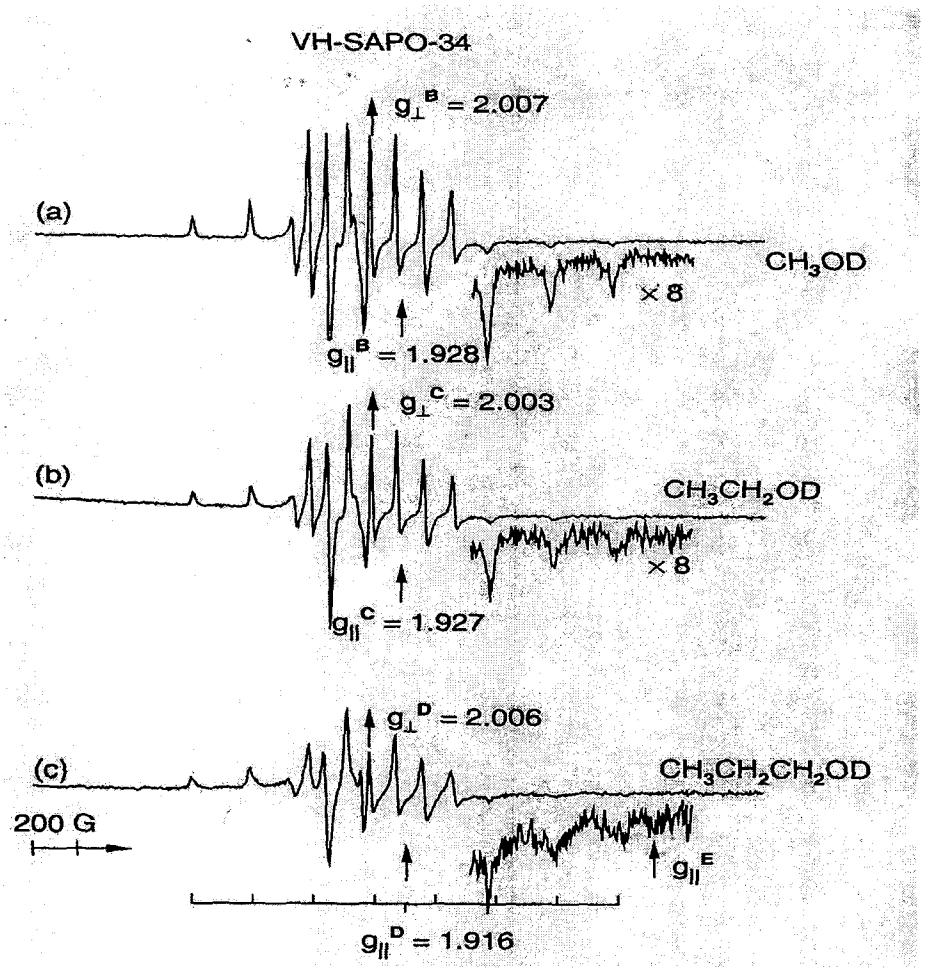

Fig. 5. EPR spectra at 77 K of activation VH-SAPO-34, after adsorption of CH_3OD at room temperature for 20 min, (b) after adsorption of CH_3CH_2OD at room temperature for 20 min, and (c) after adsorption of $CH_3CH_2CH_2OD$ at room temperature for 44 min.

EPR measurements

Table 1. EPR Parameters at 77 K of paramagnetic Ion Species,Pd(I) and V(IV) after various adsorbate Treatments in H-SAPO-34.

H-SAPO-34					
Pretreatment Activated Species:Adsorbate Site	g_{II}	$g_{\perp}$	activated species : adsorbate Site	g_{II}	$g_{\perp}$
Pd^{+} : III	2.92	2.177			
Pd^{+} : IV	2.92	2.136			
Pd^{+} : I	2.92	2.070	V(IV)O : I	1.906	2.016
O_2 or H_2O : Pd^{2+}- O_2^{-} : I or IV	1.988 1.963	2.048	V(IV)O-H_2O : I	1.930	2.009
+NH_3 Pd^{2+}-NH_3 : I or IV	2.92	2.12	V(IV)O-NH_3 : I	1.955	2.023
+CH_3OH Pd^{+}-CH_3OH : I	2.676	2.132	V(IV)O-CH_3OH	1.928	2.007
+CH_3CH_2OH Pd^{+}-EtOH : I	2.048	2.095	V(IV)O- ETOH : I	1.927	2.003
$CH_3CH_2CH_2OH$ Pd^{+}-PrOH : I	2.048	2.095	V(IV)O-PrOH : I	1.916	2.006
+C_2H_4 Pd^{+}-C_2H_4 : I	2.256	2.004	V(IV)O-C_2H_4 : I	1.905	2.019
+H_2 Pd^{+} : I	2.569	2.10	V(IV)O : I	1.906	2.017

Table 2. Comparison of Spin Hamiltonian Parameters of VO^{2+} and V^{4+} in Several Matrices.

System	Vanadium species	Site symmetry	T(K)	g_{II}	$g_{\perp}$	A_{II}	$A_{\perp}$	Ground state	ref
GeO_2 amorphous	VO^{2+}	Octahedral	300	1.929	1.976	175	68	d_{xy}	25
$VOPO_4.2H_2O$	VO^{2+}	Octahedral	300	1.938	1.981	174	64	d_{xy}	26,27
V_2O_5/TiO_2	VO^{2+}	Octahedral	77++	1.909	1.973	170	-	d_{xy}	a
V_2O_5/SiO_2	VO^{2+}	Octahedral	300	1.941	1.996	179	70	d_{xy}	19
V_2O_5/Al_2O_3	VO^{2+}	Octahedral	300	1.946	1.987	177	65	d_{xy}	19.28
$VOSO_4$/SAPO-34	VO^{2+}	Octahedral	300	1.906	2.016	191	86	d_{xy}	This work
V_2O_5/SAPO-34	VO^{2+}	Octahedral	300	1.905	2.015	191	85	d_{xy}	"
$ThSiO_4$	V^{4+}	Tetrahedral	77&	1.844	1.985	164	33	d_{xy}	29
SiO_2/ Crystovalite	V^{4+}	Tetrahedral	77&	1.942	1.987	98	42	d_{xy}	30
$Ca_3ScSi_3O_{12}$	V^{4+}	Tetrahedral	77&	1.852	1.981	155	33	$d_{x^2-y^2}$	31,32
TiO_2	V^{4+}	octahedral	77++	1.956	1.912 1.915	142	43 31	$d_{x^2-y^2}$	33

Units of 10^{-4} cm^{-1} & Spectrum cannot be observed at 300 K. ++Spectrum can also be observed at 300 K. References : (a) E. Servica and R. N. Schindler *Z. Naturf.* **36a**, 992 (1981)

The g values were determined by the method described in the previous paper.[28]

G_{II} values can be determined directly from the spectra with good accuracy. The first four $g_{\perp}$ values were obtained by averaging $g_{\perp}$ values between the first $g_{\perp}$ value and the eight $g_{\perp}$ value. The other three $g_{\perp}$ values were obtained by the same procedure yielding the fist $g_{\perp}$ value. Table 1 summarizes the EPR parameters of the various paramagnetic V species observed with various adsorbates in VH-SAPO-34, compared with those from previous work on PdH-SAPO-34.[34] Table 2 summarizes the g factors of the two vanadium species(VO^{2+}, V^{4+}) observed in various matrices including the present work in SAPO.

Thermal Reduction

After solid-state reaction between as-synthesized SAPO-34 and $VOSO_4.XH_2O$, the fresh hydrated sample remains white and both EPR spectra show a powder type EPR signals. Figure 1a shows the EPR spectrum of a fresh hydrated sample. The sample was white after the subsequent oxidation treatment with static dry oxygen under 230 Torr kept at 500 °C for 3.5 h. Degassing of the sample at room temperature produces a dehydrated sample which is light gray color. Dehydration near 300 °C for 2 h begins to form a weak ESR signal and the sample becomes light gray. The EPR intensity of the dehydrated sample after the treatment was reduced to one-tenth compared with that of a activated sample. The oxidized light gray sample produces powder-type EPR signals as shown in Fig. 1b. When a dehydrated sample was evacuated by increasing temperature gradually up to 500 °C for 10 h to give an activated sample, the sample turned from light gray to gray. The activated sample has almost the same EPR signals as a dehydrated sample except with much increased signal intensity, as show in Figure 1b and 1c. The paramagnetic V-signal of the dehydrated sample showed a decrease to about one- or two-tenth of that for an activated sample(Figure 1c). The second V(IV) species observed as minor after thermal treatment at 500 °C is also seen in the Figure 1c. The species is characterized by $g_{\perp}^{A2}$; These first signals of V(IV) with g_{II} value of 1.906 and denoted and $g_{\perp}$ value of 2.016 were observed and assigned to V(IV)O according to an isotropic EPR spectrum of the activated sample at 300 K by thermal reduction.[22] (see Figure 6a)

Adsorption Interaction

The EPR spectra of activated VH-SAPO-34 after CH_3OD, C_2H_5OD, C_3H_7OD adsorption are shown in Figure 5.

A new species denoted as B in Figure 5, which is considered to be a complex with methanol have the EPR parameters of g_{II} = 1.928 and $g_{\perp}$ = 2.007, as shown in Figure 5a. When methanol was adsorbed on an activated sample surface at room temperature, the EPR intensity for overall V(IV) species increased with the production of the A species which were observed in activated sample in Figure 1. Adsorption of C_2H_5OD on a activated sample produced a new species C, with the EPR parameters of g_{II} = 1.927 and $g_{\perp}$ = 2.003 as shown in Figure 5b. Upon the adsorption of propanol on an activated sample, the pattern of EPR spectrum was similar to that after adsorption of methanol. The $g_{\perp}^{A2}$ species was disappeared

immediately by the adsorption of polar adsorbates, such as D_2O, CH_3OD, CD_3OH, CH_3CH_2OD on the activated sample because $g_\perp^{A2}$ species were more reactive to polar molecules than that of $g_\perp^{A1}$ species. The shoulder in Figure 6 was assigned to the anion radicals of oxygen, O^- and O^{2-}, adsorbed on the surface of VO^{2+}[40a] since the interaction with polar molecules displaces the oxygen radicals from the coordination sphere of the surface ions.[41b,c] However, the interaction of nonpolar molecules like C_2D_4 with $g_\perp^{A1}$ and $g_\perp^{A2}$ species did not show any differences in EPR spectra. The EPR spectra of the sample with adsorbed C_2D_4 are shown in Figure 6b. Some important characteristic features observed in the EPR signals of VH-SAPO-34 during the adsorption process of polar molecules are (1) for all four samples a decrease in the A value of about 6 G is noted ; (2) the shoulders indicating both the hydrated sample and dehydrated sample were disappeared. The EPR spectra of activated VH-SAPO-34 after the adsorption of H_2, C_2D_4 and $^{14}ND_3$ are shown in Figure 6. When 50 Torr of dry H_2 gas was added to an activated VH-SAPO-34 at 500 °C for 27 min, the intensity of V(IV) in EPR spectra was decreased to about 80 % of the original signal, suggesting the further reduction by H_2. The shoulder indicating the dehydrated sample did not disappear after nonpolar H_2 adsorption. When ethylene added to an activated sample at room temperature, the two V(IV) species observed as a minor. These new species, $g_\perp^{G1}$ and $g_\perp^{G2}$, were observed with EPR parameters of $g_\perp^{G1}$ = 2.019 and $g_\perp^{G2}$, as shown Figure 6b. The new H species were also found after NH_3 adsorption with g_{II} = 1.955 and $g_\perp$ = 2.001, as shown in Figure 6c.

ESEM measurement

The results for ESEM simulation of VH-SAPO-34 are summarized and compared with those of Pd(I)-doped SAPO-34 in Table 3.

Figure 7 shows the three-pulse ESEM spectrum obtained at magnetic fields corresponding to the parallel component for an activated sample with adsorbed D_2O.

Deuterium modulation is clearly observed in a D_2O-adsorbed sample and V(IV) interacts with one molecule of D_2O in VH-SAPO-34 at a distance of 0.40 nm. V(IV)-D distance is shorter than that of Pd-D by 0.03 nm in PdH-SAPO-34.[34] Although this indicates a weak interaction of water molecules because of much greater distance than that of direct coordination to water(D_2O), the distance obtained by ESEM are longer by 0.05 nm than V-H distance of the axial water of structure in $VO(H_2O)_5^{2+}$ determined from the dipolar hyperfine splitting in **ESEM** and **ENDOR** measurement.[39] The samples with adsorbed CH_3OD and CD_3OH show ^2D modulation as shown Figure 8a,b.

The ESEM simulation for CH_3OD shows one deuterium nucleus at 0.30 nm from V(IV). The simulation of the ESEM signal from CD_3OH gives three deuterium nucleus at a distance of 0.35 nm. V(IV)-D distance are shorter than that of Pd(I)-D by 0.04 nm in PdH-SAPO-34.[34] indicating the V(IV) interaction with one molecule of methanol in VH-SAPO-34. The V-D distances for both V_2O_5 and $VOSO_4$ of SAPO-34 estimated by ESEM simulation for CH_3CH_2OD are quite similar each other within a range of 0.03 nm(see Figure 9), indicating V(IV) interaction with one molecule of ethanol in VH-SAPO-34.

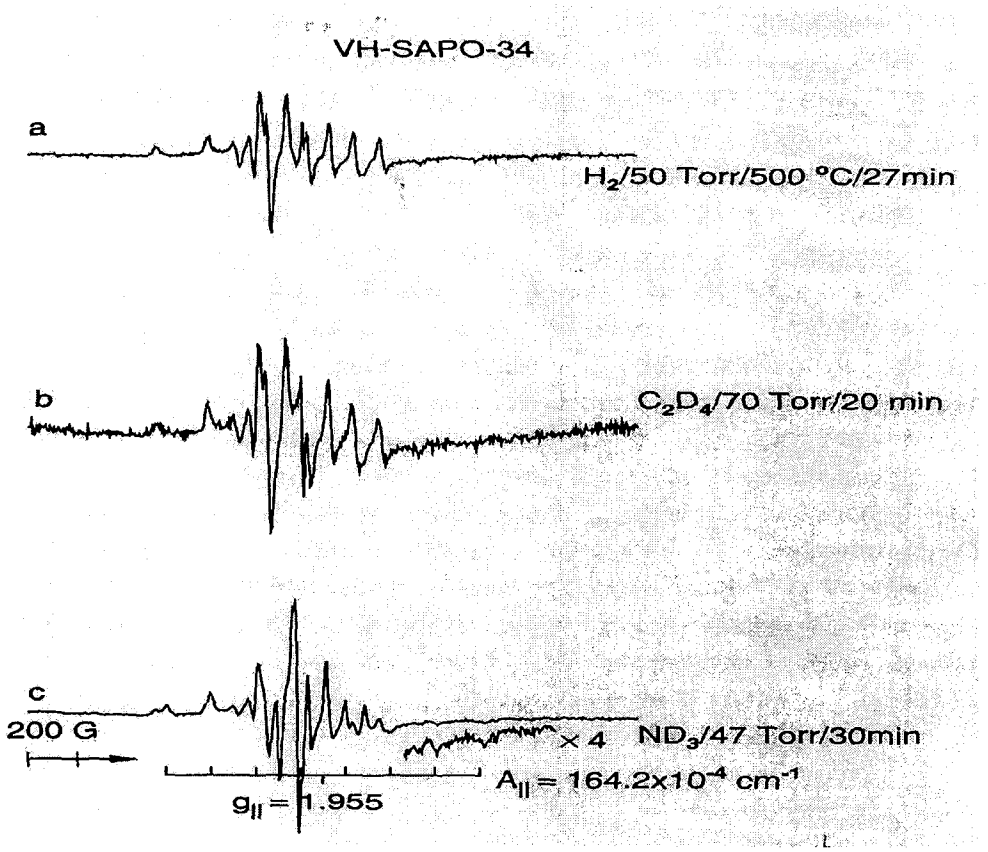

Fig. 6. EPR spectra at 300(a) and 77 K(b,c) of activated VH-SAPO-34, (a) after adsorption of 50 Torr of dry hydrogen at 500 °C for 27 min, (b) after adsorption of 70 Torr C_2D_4 at room temperature for 20 min, (c) after adsorption of 47 Torr of $^{14}ND_3$ at room temperature for 30 min

Table 3. ESEM Parameters for Pd(I) and V(IV) with Various Adsorbates in H-SAPO-34

	Pd(I)			V(IV)		
adsorbate	N[a]	R[b]	N(MHz)	N[a]	R[b](nm)	A[c](MHz)
D_2O	4	0.43	0.13	2	0.40	0.36
CD_3OH	3	0.39	0.18	3	0.35	0.09
CH_3OD	1	0.30	0.23	1	0.30	0.16
CH_3CH_2OD				1	0.29	0.23
$CH_3CH_2CH_2OD$				1	0.37	0.23
C_2D_4	4	0.39	0.12	4	0.36	0.14

[a]Number of deuterium nuclei, [b]Distance between V(IV) or Pd(I) and deuterium : estimated uncertainty is ± 0.01 nm. [c]isotropic hyperfine coupling constant : estimated uncertainty is ± 10%.

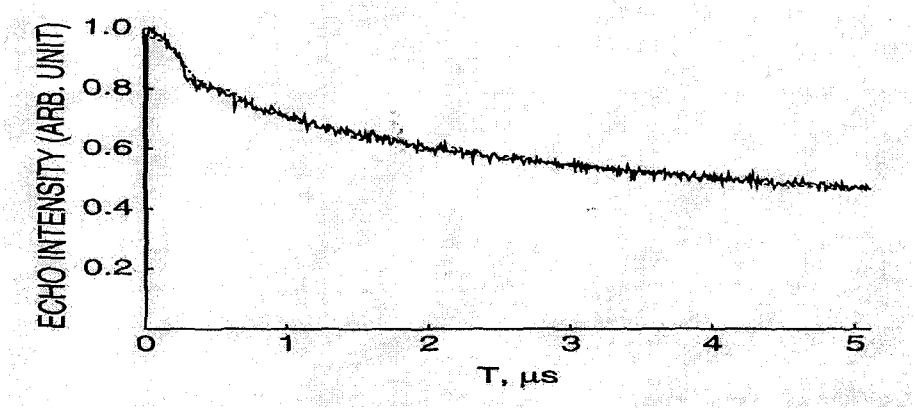

Fig. 7. Experimental(-) and simulated(---) three pulse ESEM spectra at 4 K of activated VH-SAPO-34 exposed to room temperature vapor pressure of D_2O for 20 min at a magnetic field corresponding to the parallel component(N = 2, R = 0.40 nm and A = 0.36 MHz)

(a)

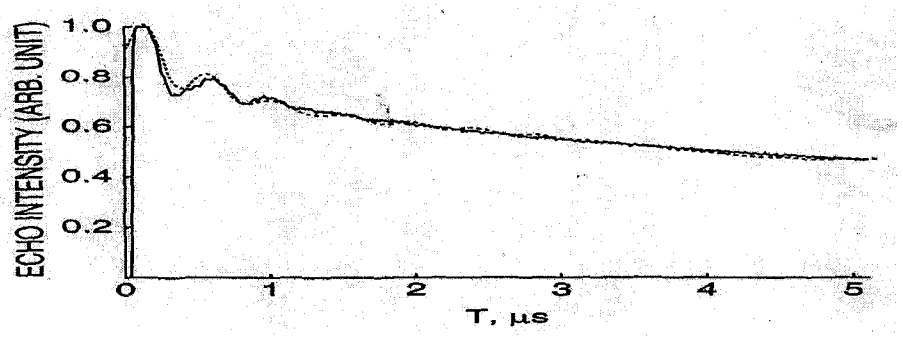

(b)

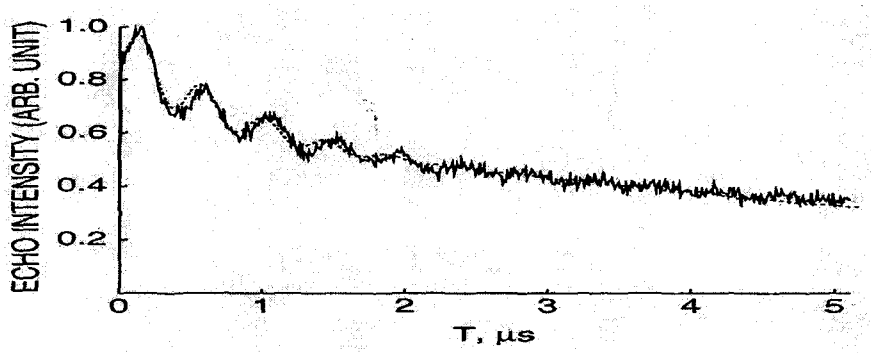

Fig. 8. Experimental (-) and simulated (---) three pulse ESEM spectra at 4 K of activated VH-SAPO-34, (a) with adsorbed CH_3OD (N = 1, R = 0.30 nm, A = 0.16 MHz) and (b) with adsorbed CD_3OH (N = 3, R = 0.35 nm, A = 0.09 MHz).

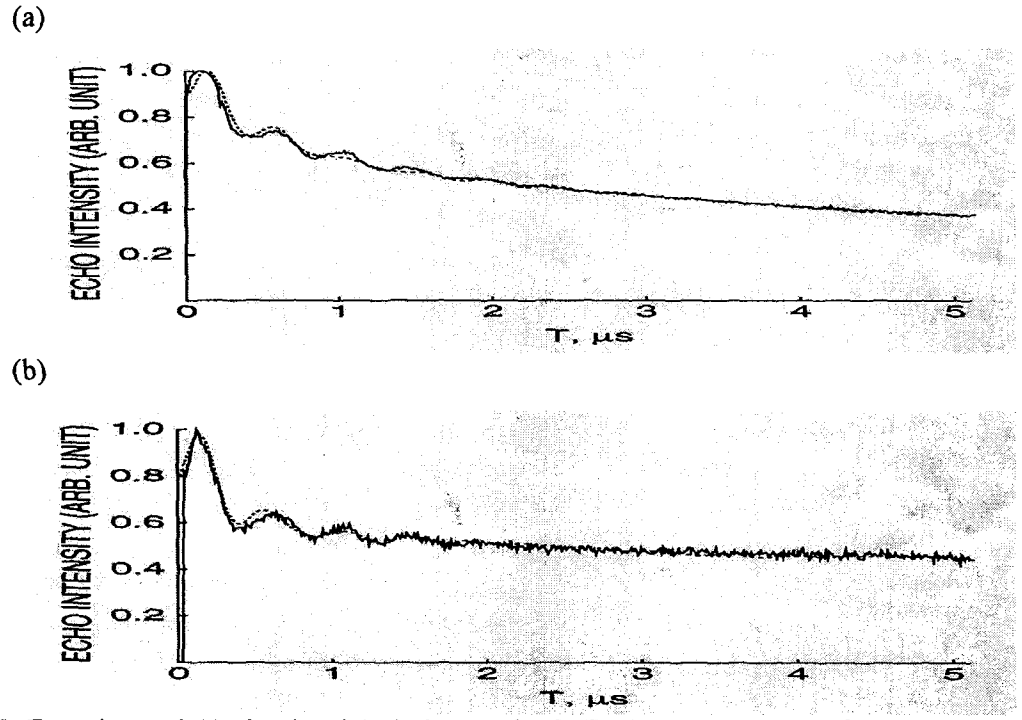

Fig. 9. Experimental (-) simulated (---) three pulse ESEM spectra at 4 K of activated VH-SAPO-34 exposed at room temperature vapor pressure of CH_3CH_2OD (a) the sample of $VOSO_4XH_2O$ and as-synthesized SAPO-34 (N = 1, R = 0.29 nm, A = 0.23 MHz) (b) the sample obtained by solid state reaction of V_2O_5 and as-synthesized SAPO-34 (N = 1, R = 0.26 nm, A = 0.23 MHz).

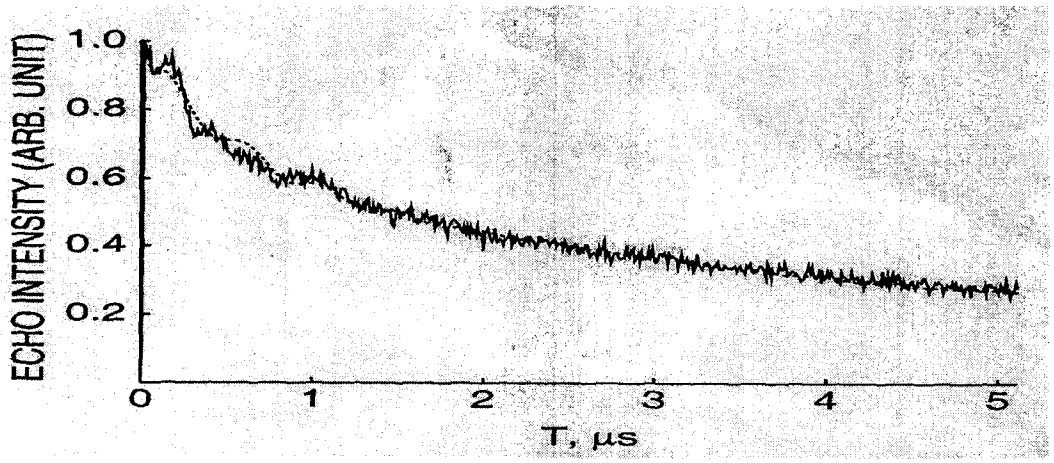

Fig. 10. Experimental (-) and simulated (---) three pulse ESEM spectra of 4 K of activated VH-SAPO-34 exposed to 50 Torr of C_2D_4 for 20 min at a magnetic field corresponding to the perpendicular component of species g (N =4, R = 0.36 nm, A = 0.14 MHz)

The three-pulse ESEM spectrum of VH-SAPO-34 with adsorbed ethylene was somewhat noisy and best simulated by four deuterium nuclei at 0.36 nm with A_{iso} = 0.14 MHz, but the parameters seem to be consistent with the interaction between a π-bonding interaction of V(IV) and one ethylene molecule(see Figure 10).

V(IV)-D distance is somewhat shorter than that of Pd(I)-D by 0.03 nm in PdH-SAPO-34. Two shell model was required for the best fit simulation of a ESEM signal for a sample after the adsorption with ethanol or propanol. The simulation parameters suggest that one ethanol and propanol molecule are coordinated indirectly to V(IV) at a distance of 0.29 and 0.37 nm, respectively(see Figure 9a, 11).

However, the ESEM results for Cu-doped sample of CuH-SAPO-34 suggest that two ethanol molecules are coordinated to the Cu(II) ion at a distance of 0.28 nm, while a third molecule is coordinate to Cu(II) at a distance of 0.32 nm.[42]

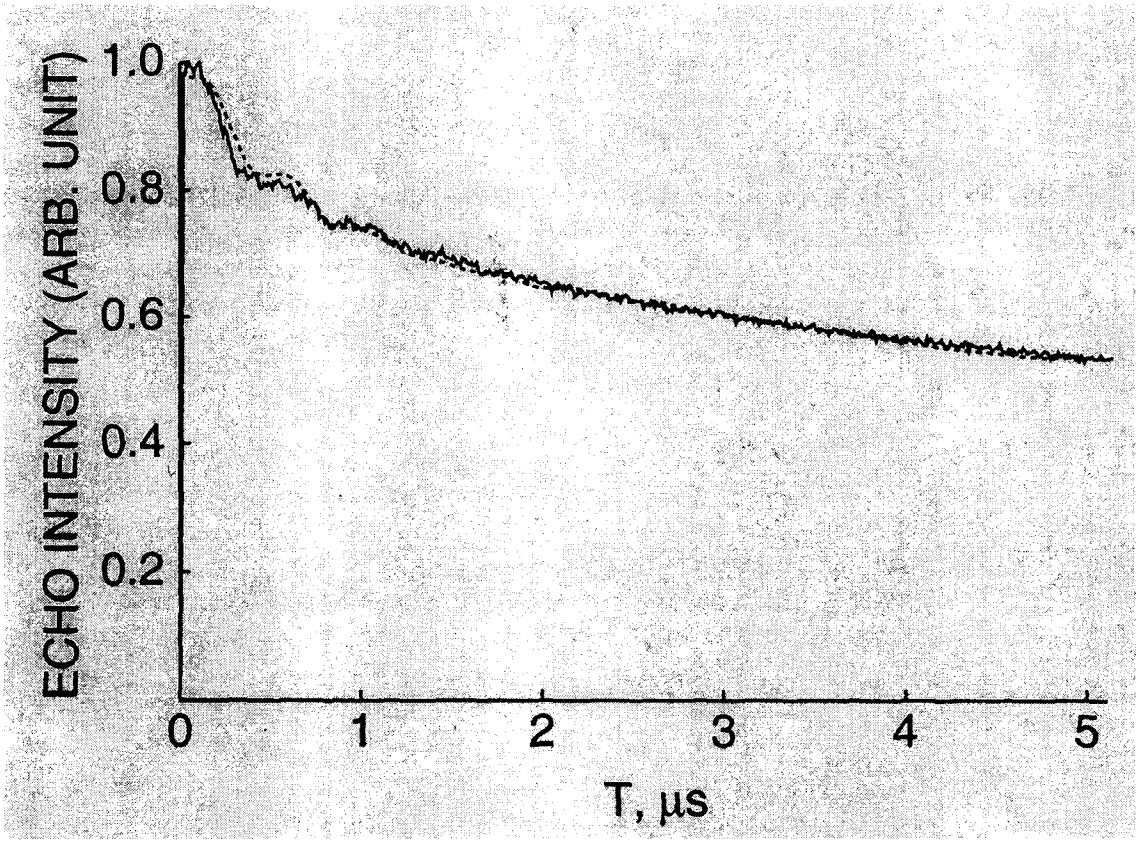

Fig. 11. Experimental(-) and simulated(---) three pulse ESEM spectrum at 4 K of activated VH-SAPO-34 exposed to room temperature vapor pressure of $CH_3CH_2CH_2OD$ for 45 min at a magnetic field corresponding to the perpendicular component of species D (N =1, R = 0.37 nm A = 0.23 MHz).

DISCUSSION

The H-SAPO-34 molecular sieve has a framework similar to that of the naturally occurring zeolite, chabazite.

The framework of SAPO-34 consists of distorted hexagonal prisms linked together by four-membered rings to form a large ellipsoidal cavity. Each ellipsoidal cavity is interconnected with six identical cavities through an eight-membered oxygen ring with an opening diameter of about 0.44 nm, by analogy with the cation site of chabazite zeolite, position location of cation sites SAPO-34 have been proposed;[34] site I is displaced from a six-ring into the ellipsoidal cavity, site II is located near the center of the ellipsoidal cavity, site III is assigned to the center of the hexagonal prism, and site IV is near an eight-ring window. Figure 12 illustrates the unit cell of SAPO-34 along with the designated cation sites.

The most common oxidation states of vanadium species showing paramagnetic properties are V(IV) and V(III) whose electronic configuration are $3d^1$,$3d^2$, respectively. Tetravalent vanadium occurs as V^{4+} or as a stable oxo-vanadium molecular ion VO^{2+}.

The ion in tetrahedrally coordination generally has a very short spin-lattice relaxation time (T_1) because of low lying excite state. Thus its EPR spectra can only be observed at or below 77 K.[22] In sharp contrast the molecular VO^{2+} species generally forms in pyramidal or distorted octahedral coordination and has a long T_1. So the ir-resolved EPR spectra can be measured even at room temperature. V^{4+} and vanadyl cation that has a low negative frame-

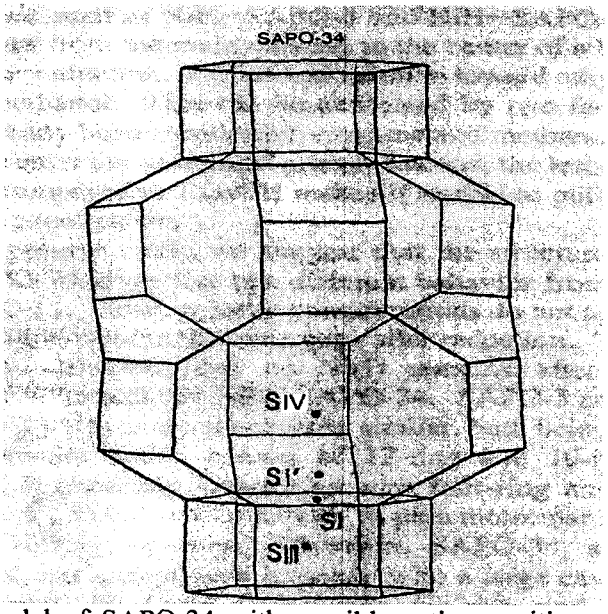

Fig. 12. Structural model of SAPO-34 with possible cation position shown. The roman numerals indicates cation sites (adopted from ref. 43).

work charge,[35] can be stabilized in SAPO-34, while more positive charged species like V^{4+} are not easily stabilized. Similar results were obtained in Pd-exchanged[36-37] SAPO-34 molecular sieve,[34] Mo-exchanged SAPO-5, and SAPO-11 molecular sieve.[38] Since the EPR signals of an oxidized sample are identical to those of an active sample, the paramagnetic V-signals observed in an oxidized dehydrated sample are also suggested to be due to vanadyl ion VO^{2+}.

Site location of A_1 and A_2 Species

The presence of two different A species indicates that there are at least two possible different location for vanadyl ion[V(IV)]O^{2+} in activated VH-SAPO-34 molecular sieve. The previous paper[34] reported three sites for Pd(I) in PdH-SAPO-34 and suggested site IV as the most accessible, site I as intermediately accessible and site III as the least accessible. Adsorption of H_2 on activated VH-SAPO-34 decreases the overall intensity of the V(IV) signals, probably owing to further reduction(Figure 6a). The perpendicular component of species A_2 did not disappear. However, $g_{\perp}^{A2}$ was disappeared by the adsorption of polar adsorbates, such as D_2O, CH_3OD, CH_3CH_2OD, and NH_3 on the activated sample. Upon adsorption of O_2 at 0.5 Torr, A_2 species doesn't disappear. A_2 species assigned to the anion radicals of oxygen O^- and O^{2-}, was adsorbed on the surface of VO^{2+},[41a] since the interaction with polar molecules displaces the oxygen radicals from the coordination sphere of the surface ions.[41b,c] Since zero or one silicon nuclei are expected in a six-ring window it is most likely that vanadium ions are located near a six-ring window with three Al nuclei, two P nuclei and one Si nucleus, or at the center of a double six-ring with Al nuclei, five to four P nuclei and one to two Si nuclei.

The previous paper [34] suggested that the palladium(I) exist in three position, six-ring window, eight-ring window and in the center of a double six-ring. Within a restricted space such as a cage in SAPO molecular sieves, the coordination of such oxo-vanadium species can differ from that of Pd(I) which is expected to be in a typical cation site in SAPO material, namely coordinated to be a 6-ring window in the ellipsoidal cavity. Therefore, it is likely that the positive charged vanadyl ion will locate near a negative charged six-ring window with at least one silicon substituted for phosphorus. This site can be identified as sit I in the chabazite cage near a six-ring window (Figure 12). Similar behavior has been reported in NiH-SAPO-34.[43] However, migration of metal ions from super cages and larger channels to smaller ones during dehydration is a common phenomenon in other molecular sieves. [44]

Adsorbate Coordination Structure

Van Reijon and Cosse[12] proposed that the initial calcined V_2O_5/SiO_2 system contains $(VO_4)^{4-}$ units which charge into $(VO)^{2+}$ in square-pyramidal coordination on interaction with NH_3 or H_2O. These adsorbates with CH_3OD, CH_3CH_2OD, $CH_3CH_2CH_2OD$ facilitate the migration of the V(IV) cation into a single location. Upon the adsorption of these polar adsorbent to the activated VH-SAPO-34, the migration of the $(VO)^{2+}$ from six-ring window

and eight ring window moved to near the ellipsoidal cavity from the original six-ring window occurs. $V(IV)O^{2+}$ ion after the exposure to these adsorbates locates in a most probable site I. Z. Maggie et al. [42] suggested that the location of Cu(II) after exposure to these adsorbates is site I. The analysis of deuterium modulation from the ESEM signal upon the adsorption the ethylene indicates that $V(IV)O^{2+}$ ion interacts with four deuterium at a distance of 0.47 nm(see Figure 11). The interaction of $V(IV)O^{2+}$ with four deuterium suggests that the ethylene molecule interacts with the V(IV)O cation with molecular plane perpendicular to a line toward the $V(IV)O^{2+}$ ion. Cu(II) ion doped in H-SAPO-34 has a similar ethylene orentaton.[42]

CONCLUSION

A solid reaction of $VOSO_4.H_2O$ and V_2O_5 with as-synthesized SAPO-34 generates paramagnetic V(IV) species. Further subsequent oxidation results weak paramagnetic V(IV) species in EPR spectra and the additional activation makes the formation of V(IV) species. The EPR and ESEM data indicate that the V(IV) species exist as a vanadyl ion either as $[V(IV)]O^{2+}$ or V^{4+} (Figure 13). The $[V(IV)]O^{2+}$ species seems to be more probable because SAPO-34 having a low negative framework charge[35] and more positively charged species like V^{4+} can not be easily stabilized. Tetravalent vanadium ion in vanadium-doped SAPO-34 can only be observed at the temperature lower than 77 K, while the vanadyl ion VO^{2+}, the activated sample of VH-SAPO-34 can produce the ion even at room temperature. After the adsorption of methanol, ethanol, propanol or ethane to the VH-SAPO-34, only one molecule coordinate to $[V(IV)]O^{2+}$ was observed in EPR and ESEM spectra.

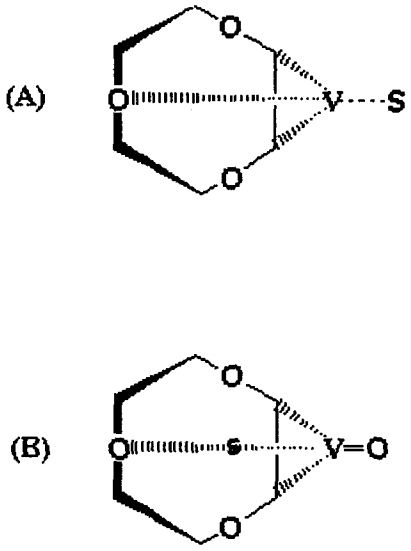

Fig. 13. Possible vanadium species on the surface of SAPO-34 molecular sieves: (a) tetravalent vanadium species (b) oxovanadium species (s:solvent).

REFERENCES

1. S. T. Wilson, B. M. Lok, C. A. Messina, T. R. Cannan and E. M. Flanigen, *J. Am. Chem. Soc.*, **104**, 1146 (1982).
2. B. M. Lok, C. A Messina, R. L. Patton, R. T Gajek, T. R.Cannan aqnd E. M. Flanigen,*J. Am. Chem. Soc.*, **106**, 6092 (1984).
3. R. Szostak, Molecular Sieves ; *Principle of Synthesis and Identification,* Van Nostrand Reinhold ; NewYork, 1989 Chap 4.
4. (a) B. M. Lok, C. A. Messina, R. L. Patton, R. T. Gajek, T. R. Cannan and E. M. Flanigen, *U. S. Pat.* 4400871, (1984) (b) B. M. Lok, C. A. Messina, R. L. Patton, R. T. Gajek, T. R. Cannan and E. M. Flanigen, *J Am. Chem. Soc.*, **106**, 6092 (1984).
5. M. S. Wain and N. R. Foster, *Cat. Rev-Sci.* Eng. **19**, 211 (1979).
6. G. C. Bond, *J. Catal.* **8**, 149 (1989).
7. A. J. Van Hengstum, J. G. Van Ommen, H. Bosch and P. Gellings, *J. Appl. Catal.* **8**, 369 (1983).
8. H. K. Matralis, Ch. Papadopoulou, Ch. Kordulis, A. A. Elguezabal and V. C. Corberan *Appl. Catal. A* **126**, 365 (1995).
9. F. Nakajima, and I. Hamada, *Catal. Today* **29**, 109 (1996).
10. H. Bosch and F. Janssen, *Catal. Today* **2**, 369 (1988).
11. G. C. Bond and S. Flamerz-Tahir, *Appl. Catal.* **71**, 1 (1991).
12. L. L. Van Reijen and P. Cosse, *Dicuss. Faraday Soc.*, **41**, 277 (1966).
13. K. Mori ; A. Miyamoto, A. T. Ui and V. Murami, *J. Chem. Soc., Chem. Commun*, 260 (1982).
14. K. Hirota , Y. Kera and S. Teratani, *J. Phys. Chem.*, **72**, 3133 (1968).
15. A. Miyamoto, Y. Yamazaki, T.Hattori, M. Inamata and Y. Murakami, *J. Catal.*, **74**, 144 (1982).
16. V. A. Shvets, M. F. Saricheu and V. B. Kazansky, *J. Catal.*, **11**, 378 (1968).
17. V. M. Vorotynsev, V. A. Shvets and V. B. Kazansky, *Kinet. Katal.*, **12**, 678 (1971).
18. H. J. Sung, S. U. Young and H. Chon, *Appl. Catal.*, **62**, 61 (1990).
19. M. Narayana, C. S. Narashimhan and L. Kevan, *J. Chem. Soc., Faraday Trans.*, **81**, 137 (1985).
20. Y. Xu, P. J. Maddox and J. W. Couves, *J. Chem. Soc., Faraday Trans.*, **86**, 425 (1990).
21. M. Zamadics, X. Chen and L. Kevan, *J. Phys. Chem.*, **96**, 2652 (1992).
22. M. Narayana and L. Kevan *J. Phys. C : Solid State Phys.*, **16**, L863 (1983)
23. Kevan, L. In *Time Domain Electron Spin Resonance,* eds. L. Kevan and R. N. Schwarz, 279-341 Chapter 8., Wiley ; New York, 1979.
24 S. A. Dikanov, A. A. Shubin, and V. N. Parmon, *J. Magn. Reson.*, **42**, 474 (1981).
25. I. Siegel, *Phys. Rev.*, **134**, A193-7 (1964).
26. Ballutaud D. ; D. Bordes E. and Courtine P. *Mater. Res. Bull.*, **17**, 519-26 (1982).
27. Ballutaud D. ; Bordes E. and Schinder R. N., *Z. Naturf.*, **36a**, 992-5 (1981).
28. Inomata M. ; Mori K. and Murakami Y., J. Phys. Chem., **87**, 761-8 (1983).

29. Di Gregorio S, Green Blatt M, Pifer J. H. and Sturge M. D. *J. Chem. Phys.*, 2931- 7 (1982).
30. Grunin V. S., *Sov. Phys.-Solid State*, **12**, 1785-8 (1971).
31. Havichek V. and Novak P. Czech, *J. Phys. Status Solidi*, **B24**, 189-203 (1974).
32. Havicek V. and Novak P. Czech, *J. Phys. Status Solidi*,, **B64** K19-23 (1974).
33. H. J. Garritsen and H. R. Lewis, *Phys. Rev.* **119**, 190 (1960).
34. G. H. Back, J. S. Yu, V. Kurshev and L. Kevan, *J. Chem. Soc., Faraday Tras.*, **90**(15), 2283 (1994).
35. E. M. Flanigen, B.M. Lok, R. L. Patton and S. T. Wilson, *Pure Appl. Chem.*, **58**, 1351 (1986).
36. T. Saint-Pierre, X. Chen, and L. Kevan, *J. Phys. Chem.*, **97**, 932 (1993).
37. C. W. Lee, J. S. Yu and L. Kevan, *J. Phys. Chem.*, **96**, 7747 (1992).
38. C. W. Lee, T. Saint-Pieere, N. Azuma and L. Kevan, *J. Phys. Chem.*, **97**, 11811 (1993).
39. D. Suryanaraanar, P. A. Narayana and L. Kevan, *J. Phys. Chem.*, **86**, 4579 (1982).
40. (a) D. Kivelson and S. K. Lee, *J. Chem. Phys.*, **41**, 1896 (1964).
(b) D. Kibelson, ibid., **33**, 1094 (1960) (c) D. Kivelson, ibid, **27**, 1087 (1957).
41. (a) M. Ya, Kon, and V. A. Shvets, *Kinetica Kakaliz*, **13**, 735 (1972).
(b) V. M. Vorotyntsev, V. A. Shvets and V. B. Kazanskii, ibid, 12, 793 (1971).
(c) V. A. Shevets and V. B. kazanskii, ibid, **12**, 924 (1971).
42. M. Zamadics, X. Chen and L. Kevan, *J. Phys. Chem.*, **96**, 5488 (1992).
43. M.. A. Dijeugoue, A. M. Prakash, and L. Kevan, *J. Phys. Chem.* B, **102**, 4386 (1998)
44. W. M. H. Sachtler, Z. Zhang. *Adv. Catal.* **39**, 129 (1993).